Eur Spine J (2013) 22:1101–1112
DOI 10.1007/s00586-012-2644-x

ORIGINAL ARTICLE

Thoracic cage plasticity in prepubertal New Zealand white rabbits submitted to T1–T12 dorsal arthrodesis: computed tomography evaluation, echocardiographic assessment and cardio-pulmonary measurements

Federico Canavese · Alain Dimeglio · Marco Stebel · Marco Galeotti · Bartolomeo Canavese · Fabio Cavalli

Received: 7 May 2012 / Revised: 19 December 2012 / Accepted: 20 December 2012 / Published online: 10 January 2013

Abstract
Purpose We aimed to describe the morphological changes in the thoracic cage and spinal column induced in New Zealand White (NZW) prepubertal rabbits subjected to dorsal arthrodesis and observed at skeletal maturity by computed tomography (CT) scans. This was done to evaluate the plasticity of the thoracic cage of rabbits with non-deformed spine, by highlighting its modifications after spinal arthrodesis. Emogas data analysis, echocardiographic assessment and cardio-pulmonary measurements completed the evaluation.

Methods Surgery was performed in 16 female rabbits, 6 weeks old. Nine were subjected to T1–T12 dorsal arthrodesis, while seven were sham-operated. Surgery involved the implant of two C-shaped stainless steel bars and heterologous bone graft. CT scans were performed before surgery, 2, 6 and 12 months after surgery. One week after the last CT scan, echocardiographic and emogas evaluations were performed.
Results Chest depth (8 %), thoracic kyphosis (ThK) (23 %), dorsal and ventral length of the thoracic spine (11 %) and sternal length (7 %) were significantly reduced in operated compared to sham-operated rabbits. Mean values ± standard deviation (SD) of $PaCO_2$, PaO_2 and sO_2 were not significantly different. Mean values ± SD of echocardiographic measurements were not significantly different between the two groups of rabbits, except for thickness of the interventricular septum in systole, contractile capacity of the left ventricle and ejection fraction.
Conclusions T1–T12 dorsal arthrodesis in prepubertal NZW rabbits with non-deformed spine induced changes of the thoracic cage morphology. However, those changes are source of cardio-pulmonary complications not severe enough to reproduce a clinical picture comparable to thoracic insufficiency syndrome in humans.

Keywords Arthrodesis · Prepubertal rabbits · CT scan · Early onset scoliosis · Cardio-pulmonary assessment

F. Canavese (✉)
Service de Chirurgie Infantile, Centre Hospitalière Universitaire Estaing, 1 Place Lucie et Raymond Aubrac, 63003 Clermont Ferrand, France
e-mail: canavese_federico@yahoo.fr

A. Dimeglio
Faculté de Médecine, Université de Montpellier, 2 Rue de l'Ecole de Medecine, 34000 Montpellier, France

M. Stebel
Department of Life Sciences, Animal Facility, Università degli Studi di Trieste, Via Valerio 28, 34127 Trieste, Italy

M. Galeotti
Veterinary Pathology Section, Department of Food Science, Università degli Studi di Udine, Via Sondrio 2, 33100 Udine, Italy

B. Canavese
Università degli Studi di Udine, Via Palladio 8, 33100 Udine, Italy

F. Cavalli
Research Unit of Paleoradiology and Allied Sciences, Azienda Ospedaliero-Universitaria, LTS, 34127 Trieste, Italy

Introduction

Children with progressive early onset spinal deformities or with extensive fusion of the thoracic spine before the age of 7 are often characterized by short stature, reduced trunk height and a disproportionate body habitus.

Cardiac and respiratory problems can develop after a precocious vertebral arthrodesis or as a consequence of pre-existing severe vertebral deformities and can vary in patterns and timing, according to the existing degree of deformity [1–6]. These deformations, which can be lethal in the most severe cases, result from mutual interactions and influences among the various skeletal and organic components of the thoracic cage and cavity that are still not well understood.

As the spinal deformity progresses, not only spinal growth is affected, but also the size and shape of the thoracic cage are modified. As a "domino effect", the distortion of the thorax will eventually interfere with lung development and cardiac function, leading those children to develop thoracic insufficiency syndrome (TIS) [3] and cor pulmonale [1] which can be lethal in most severe cases [2, 4, 5, 7–12].

The penetration of the apical portion of the deformed spine inside the thoracic cage, also called endothoracic bump, adversely affects thorax development by changing its shape and reducing its normal motility [7]. The varying extent of an experimental arthrodesis also affects differently both growth and thoraco-pulmonary functions [13–24]. Clinical data demonstrate that to develop TIS or similar clinical pictures, a significantly reduced spinal height must be present [5, 6, 13].

In this study, our experimental work aimed to describe the morphological changes in the thoracic cage and spinal column induced in New Zealand White (NZW) prepubertal rabbits, 6 weeks old, subjected to T1–T12 dorsal arthrodesis and observed at the age of 13.5 months by computed tomography (CT) scan. This was done to highlight potential cardio-pulmonary issues and the type of thoracic cage modifications after completion of skeletal growth in prepubertal rabbits with non-deformed spine subjected to dorsal arthrodesis.

Materials and methods

Animals

Sixteen prepubertal female NZW rabbits were used in this study. Nine rabbits were subjected to T1–T12 dorsal arthrodesis, while seven were sham-operated. Subjects were housed in stainless steel cages in a controlled environment (temperature of 21 °C with a relative humidity of 40–50 %, with 10–15 changes of air per hour and a light/dark cycle of 12/12 h). Cages measured 0.7 m in length, 0.43 m in height and 0.56 m in depth, and the cage volume was 0.17 m^3. Animals were fed with a standard pellet diet (2030 Global Rabbit Diet 2030, Harlan Laboratories, Indianapolis, IN, USA) and water ad libitum.

Operative procedures and animal care were performed in compliance with national and international regulations (Italian regulation D.L.vo 116/1992 and European Union regulation 86/609/EC). The protocol was examined and approved by the Director's Board of the Animal Facility of the Department of Life Sciences, University of Trieste, Trieste, Italy, prior to the start of the study. The recommendations of the ARRIVE guidelines in animals research were also consulted [25].

Anaesthesia and surgical procedure

Surgery was performed at the age of 6 weeks in all rabbits under general anesthesia (GA). GA was obtained by an intramuscular injection of xylazine 5 mg/kg (Virbaxil® 2 %, Virbac Laboratories, Carros, France) and tiletiletamine–zolazepam 15 mg/kg (Zoletil® 100, Virbac Laboratories, Carros, France). Subsequent skin analgesia was obtained with a subcutaneous injection of 2 % lidocaine hydrochloride (1 ml/animal).

Nine rabbits were operated according to a modified "Wisconsin" technique or extra canal dorsal T1–T12 vertebral arthrodesis, corresponding to posterior vertebral arthrodesis in bipeds, and seven were treated as sham-operated [26, 27]. Access to the operating area was achieved on the midline of the back between the first and twelfth thoracic first lumbar vertebrae, with a *repere* point represented by the spinous processes. Once the muscular plane had been reached, the *musculi trapezius*, *latissimus dorsi*, *spinalis thoracis* and *longissimus lumborum et thoracis* were symmetrically retracted on both sides to allow a wide exposure of the vertebral laminae, spinous and transverse processes, and the cranial and caudal *facies articulares* of the thoracic vertebrae [28]. Two specially designed C-shaped stainless steel bars of approximately 120 mm in length and 1.5 mm in diameter were positioned laterally at the base of the spinous processes of the thoracic vertebrae and fixed with multiple 2/0 non-absorbable wire ligatures. The small size of the thoracic vertebrae of a 6-week-old rabbit does not allow to bore a hole at the base of the spinous process through which the fixation wire should pass, as the original technique would require [26, 27]. Multiple fragments of heterologous bone graft (Grafton DBM®, Osteotech Inc., Eatontown, NJ, USA) were applied on each side of the spinous processes of the thoracic spine to favour fusion. The operation lasted approximately 50 min on average for each rabbit.

During the postoperative period, pain was relieved by a subcutaneous administration of carprofen (Rimadyl®, Pfizer Animal Health, West Dundee, Great Britain; 5 mg/kg twice daily for 5 days). An intramuscular injection of enrofloxacin (Baytril® 5 %, Bayer Animal Health, Kiel, Germany; 5 mg/kg twice daily) was administered for the

prevention of infection during the week following surgery. Nevertheless, some rabbits presented clinical issues (diarrheal syndrome, dehydration, weight loss) immediately and/or few days after the surgical procedure, but these were positively resolved in most cases after adequate treatment. For this reason, the surgical wound in arthrodesed animals was followed during the first 2–3 months after the intervention to avoid secondary infections. Informations provided by all those examinations are useful tools to monitor the welfare status of the subjects.

Computed tomography scan measurements

Thoracic CT scan measurements were performed on a sample of 11 rabbits. CT scan were performed immediately before surgery, 2, 6 and 12 months after surgery to obtain objective data on differences between operated and sham-operated rabbits. CT scan examinations were performed with a 16-slice CT scanner (©Aquilion 16, Toshiba Medical System Corporation, Tochigi, Japan). Tomography examinations were carried out under GA and the animals were kept supine. CT scans were examined and interpreted by the specialist to assess the positioning of the bars and ascertain whether or not bony fusion had occurred. The measures on the CT images were always carried out by the same operator to avoid interobserver error using OsiriX® Imaging software, version 3.8.1 (©Antoine Rosset, 2003–2011, Geneva, Switzerland).

Thoracic dimensions

Chest depth (CD) was calculated from the ventral face of the vertebral body to the dorsal face of the sternum. Chest width (CW) connects the inner faces of two symmetrical ribs, lies perpendicularly to CD and cuts it in half on the widest point of the thoracic cage. CD and CW were then used to obtain the thoracic index (ThI), expressed by the ratio CD/CW of the thorax. The difference between CW and CD was also calculated (CW − CD). Measurements were performed from T1 to T9. Asternal ribs start at T8 in rabbits and below this level ribs do not reach the sternum [23]. Nevertheless, T8 and T9 ribs remain regular *repere* points and thus it was possible to allow measurements until T9. Thoracic dimensions are expressed in millimeters (mm) (Fig. 1).

Thoracic kyphosis

Measurement of the degree of ThK was calculated from the upper border of T3 to the lower border of T10 according to Cobb's method [29] (Fig. 2).

Dorsal and ventral length of the bodies of thoracic vertebrae

The values of the dorsal (DL) and ventral (VL) length of individual bodies of thoracic vertebrae, respectively, were identified on the intersection line between the midsagittal and tangential planes to the vertebral body, thereby proceeding from the cranial edge to the caudal edge. The total DL (DL^{tot}) and the total VL (VL^{tot}) of the bodies of thoracic vertebrae were expressed by the sum of individual lengths. DL, VL, DL^{tot} and VL^{tot} values were expressed in mm and calculated from T1 to T12 (Fig. 3).

Sternal length

Sternal length (StL) was calculated in mm from the cranial end of the trachelian cartilage to the caudal end of the xiphoid cartilage (Fig. 3).

Body weight, blood samples, echocardiographic evaluation and cardio-pulmonary complex removal

Twelve months after the surgical intervention, the 16 rabbits were subjected to echocardiographic evaluation. The weight of each rabbit was recorded before surgery and 1, 2, 4, 7 and 12 months after surgey. One week prior to echocardiographic evaluation, all animals underwent withdrawals of blood samples from the central artery of the left ear to obtain blood gas values using the i-STAT® Portable Clinical Analyzer and the i-STAT® $CG4^{+}$ Cartridge (Abbott Diagnostics, Abbott Park, IL, USA). Rabbits were healthy at this time and free from any sign of cardiovascular or respiratory tract disease on the basis of a physical examination that included careful thoracic auscultation. Echocardiographic evaluation was performed without sedation or anesthesia with all animals in the conscious state.

Examinations were carried out with the My Lab 30 CVX Vision device (Esaote, Florence, Italy). Phased array probes PA230/3.5 MHz and convex CA123/5 MHz were used. All echocardiographic acquisitions were made in sinus rhythm and only the right parasternal view of each rabbit's hemithorax was imaged echocardiographically. Hairs were trimmed off the right parasternal region of each rabbit before echocardiographic assessment. Animals were placed in specially prepared concave basins of elastic material maintained in lateral decubitus and kept calm throughout the course of the examination. Echocardiographic evaluation was possible for all subjects and results were judged as good by veterinary ultrasonographers [30–33].

Echocardiographic values were obtained from standard feline views [34] and measurements in diastole (d) and systole (s) and included: thickness of the interventricular

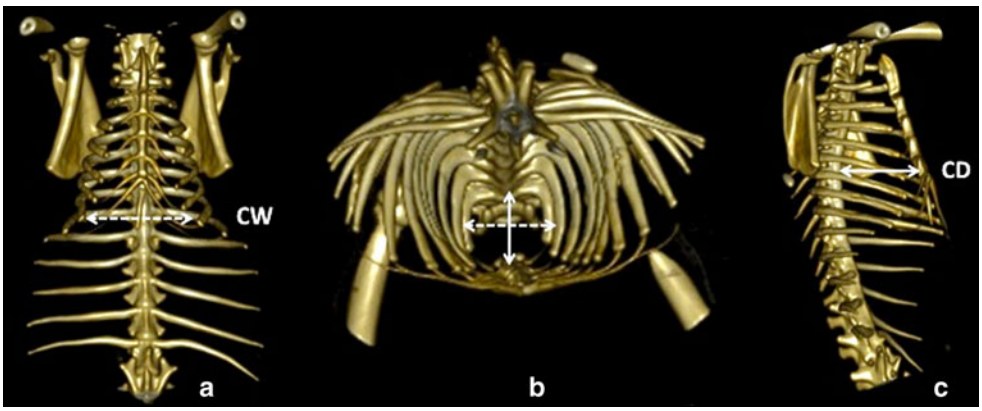

Fig. 1 Computed tomography scan with three dimensional reconstruction of the chest. Frontal view (**a**), top view (**b**) and lateral view (**c**) of the thoracic cage. *CW* chest width, *CD* chest depth

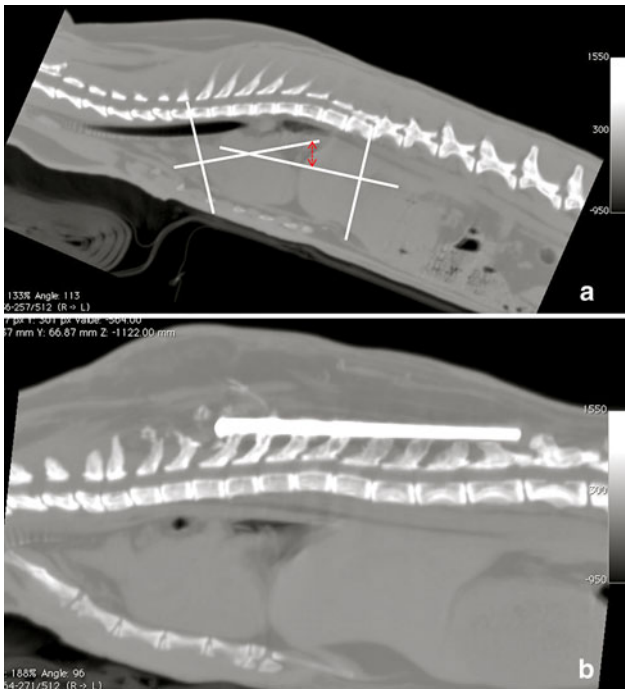

Fig. 2 Measurement of the degree of thoracic kyphosis (ThK) reduction according to Cobb's method

Fig. 3 Measurement of dorsal (DL) and ventral (VL) length of vertebral bodies, length of the sternum (StL)

septum (IVSd and IVSs) in mm; left ventricular internal diameter in mm (DVSd and DVSs); left ventricular free wall in mm (PPVSd and PPVSs); contractile capacity of the left ventricle in mm (%FS: fractional shortening defined as [100 × (DVSd − DVSs)/DVSd]); diameter of the left atrium in mm (LA); ejection fraction as a percentage (EF); diameter of the aortic wall (Ao) in mm; LA/Ao ratio. The following dynamic parameters were also recorded: maximal aortic outflow velocity (AO Vel_{Max}) in m/s; maximal aortic outflow pressure gradient (GP Ao_{Max}) in mmHg; maximal pulmonary outflow velocity in m/s (Po Vel_{Max}); maximal aortic outflow pressure gradient in mmHg (GP Po_{Max}) [30–33].

At the end of the experiment, the rabbits anesthetized with an intramuscular injection of xylazine 5 mg/kg (Virbaxil® 2 %, Virbac Laboratories, Carros, France) and tiletiletamine–zolazepam 15 mg/kg (Zoletil® 100, Virbac Laboratories, Carros, France) were euthanized with an intravenous injection of embutramide-mebenzonio-tetracaine 26 mg/kg (Tanax®, Intervet Italia Srl, Peschiera Borromeo, Italy). After death, the subjects were jugulated.

Immediately after euthanasia and jugulation, the heart–lung complex was removed. After complete removal of the whole diaphragm and removal of all ribs of the left hemithorax, the heart–lung complex was freed and detached. At this point, the heart was carefully separated from the lungs. The heart was also freed from the pericardium and the great vessels, the latter cut at their base. The lungs were separated from the parietal pleura, the right and left extra pulmonary bronchi and the great vessels. Bronchi and great vessels were cut very close to the hilus of each lung. Heart and lungs were then weighed separately and their weight was recorded in grams (g). The volume of heart and lungs was determined by displacement of an equivalent distilled water mass and values were reported in milliliters (mL).

Values were obtained from fixed specimens in 10 % buffered formalin.

Statistical analysis

Data were expressed as frequencies and percentages and means and standard deviations (SD) as appropriate. Student's t test was used for the analysis and statistical significance was set at $p < 0.05$.

Results

Body weight

Mean body weight at the day of surgery was 1,580.6 ± 134 g (range 1,429–1,875) in operated and 1,659.4 ± 109.1 g (range 1,500–1,770) in sham-operated rabbits. Mean body weight at the end of the experiment was 5,343.3 ± 497.4 g (range 4,670–6,150) in operated and 5,265.7 ± 702.9 g (range 4,440–6,100) in sham-operated rabbits. The weight of operated rabbits was corrected for the weight of metal implants (20 g). Weight of operated rabbits was 12 % less compared to sham-operated rabbits 1 month after surgery. Operated rabbits were still 7 and 5 % lighter compared to sham-operated rabbits at 2 and 7 months post surgery, respectively. Twelve months after surgery, the two groups of rabbits had nearly identical body weight. Table 1 and Fig. 4 show weight changes in operated and sham-operated rabbits.

CT scan observations and measurements

Thoracic CT scan measurements were performed on a sample of 11 rabbits (8 operated and 3 sham-operated) before surgery, 2, 6 and 12 months after surgery. Thoracic CT scan images revealed fusion of the thoracic spine occurred in 75 % of rabbits. Mean values of CD, CW, ThI, ThK, DL^{tot}, VL^{tot} and StL are shown in Figs. 5, 6, 7, 8, 9, and 10. Twelve months after surgery, and after completion of skeletal maturity, these values showed two different types of thoracic cage shape (Figs. 5, 6, 7, 8, 9, 10).

At completion of skeletal maturity, CD was reduced in operated compared to sham-operated rabbits ($p < 0.05$). Between T1 and T9, the CD reduction was 8 % on average.

ThI was also lower in operated compared to sham-operated rabbits. At skeletal maturity, the ThI reduction between T1 and T9 was 11 % on average. Similarly, the

Table 1 Mean values ± SD of body weight during the experiment

Rabbit	Before surgery	1 month	2 months	4 months	7 months	12 months
Operated						
1	1,526	1,945	3,445	4,040	4,220	4,670
2	1,525	2,435	3,530	3,920	4,680	5,610
3	1,875	2,550	3,805	4,610	4,920	5,540
4	1,640	2,445	4,100	5,120	5,740	6,150
5	1,433	2,170	3,820	4,570	5,095	4,890
6	1,570	2,480	3,940	4,920	5,490	5,550
7	1,601	1,985	3,340	3,950	4,290	5,085
8	1,626	2,430	3,790	4,500	5,170	5,770
9	1,429	2,185	3,630	4,485	5,000	4,825
Mean	1,580.6	2,291.7	3,711.1	4,457.2	4,956.1	5,343.3
SD	134.0	225.2	244.6	420.1	503.7	497.4
Sham-operated						
10	1,734	2,780	4,170	4,905	5,435	5,825
11	1,500	2,415	4,000	4,740	5,435	4,440
12	1,717	2,720	4,230	5,000	5,650	5,670
13	1,744	2,710	4,130	4,990	5,570	5,670
14	1,618	2,410	3,610	4,205	4,450	4,580
15	1,770	2,820	4,305	5,155	5,755	6,100
16	1,533	2,400	3,460	3,920	4,290	4,575
Mean	1,659.4	2,607.9	3,986.4	4,702.1	5,226.4	5,265.7
SD	109.1	190.3	325.1	461.5	597.7	702.9

Values are expressed in grams

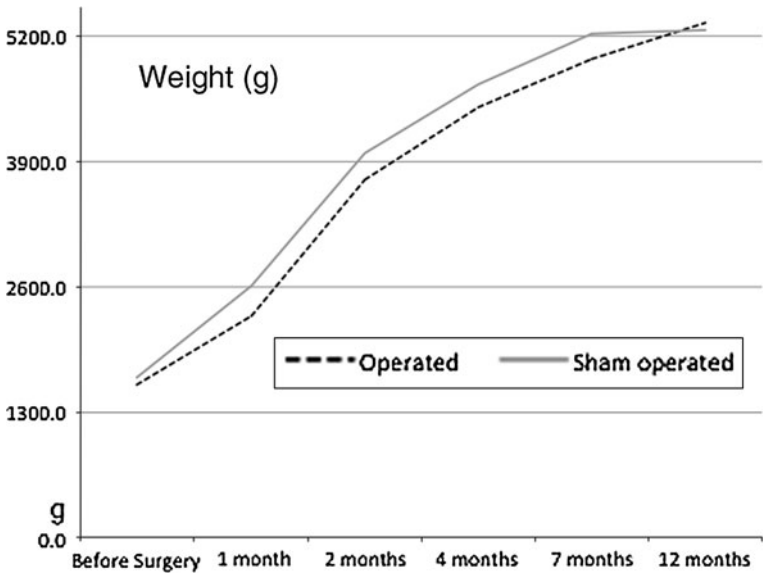

Fig. 4 Operated rabbits had reduced body weight compared to sham-operated rabbits. Twelve months after surgery, operated rabbits (*dotted line*) and sham-operated rabbits (*grey line*) showed nearly identical body weight. Weight is expressed in grams (g)

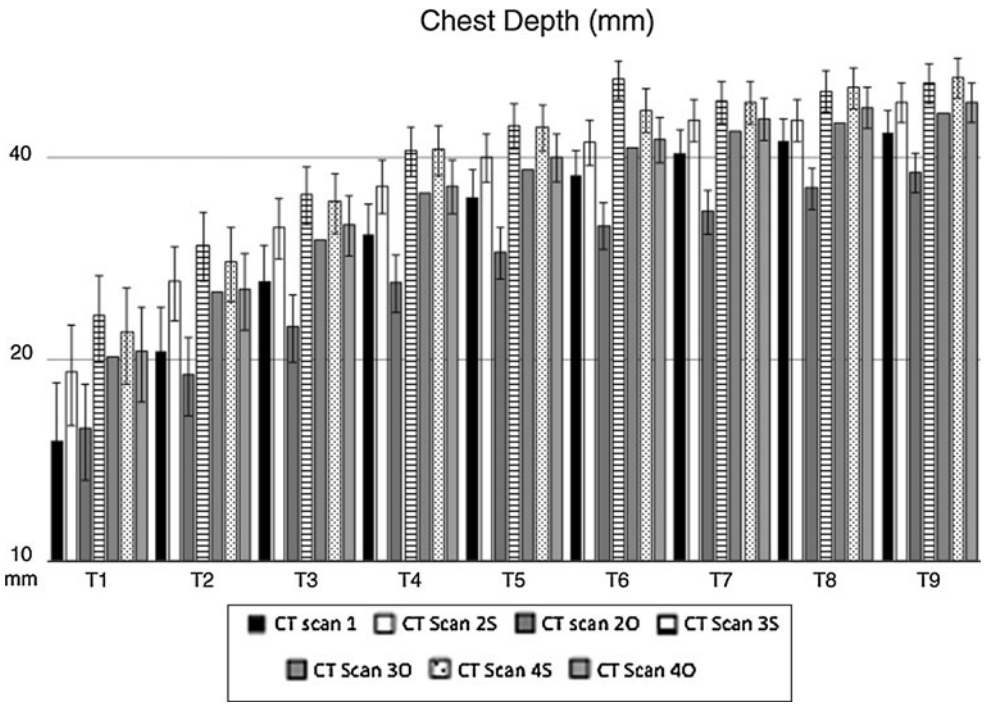

Fig. 5 Chest depth (CD) changes from T1 to T9 in operated (O) and sham-operated (S) rabbits during the experiment. Mean values are expressed in millimeters (mm). *Error bars* identifies standard error. *CT Scan 1* CD before surgery (*black column*). Operated rabbits (O): *CT Scan 2O* CD 2 months after surgery, *CT Scan 3O* CD 6 months after surgery, *CT Scan 4O* CD 12 months after surgery. Sham-operated rabbits (S): *CT Scan 2S* CD 2 months after surgery, *CT Scan 3S* CD 6 months after surgery, *CT Scan 4S* CD 12 months after surgery. At completion of skeletal maturity CD was reduced in operated compared to sham-operated rabbits ($p < 0.05$)

length of the T1–T12 spinal segment was 10 % shorted in operated compared to sham-operated rabbits ($p < 0.05$). Moreover, ThK and StL showed an average of 23 and 7 % reduction in operated compared to sham-operated rabbits ($p < 0.05$).

Blood sample analysis

Mean values ± SD of partial pressure of carbon dioxide ($PaCO_2$) in mmHg, partial pressure of oxygen (PaO_2) in mmHg, total carbon dioxide tension (TCO_2) in mEq/L, bicarbonates (HCO_3^-) in mmol/L, oxygen saturation (saO_2) as a % and pH are provided in Table 2.

Echocardiographic evaluation

Echocardiographic parameters (M-mode, 2D, Doppler echocardiography) were easily recorded in all rabbits in the conscious state. Table 3 provides mean values ± SD of echocardiographic measurements for operated and sham-operated rabbits. Values are not significantly different between the two groups of rabbits ($p > 0.05$), except for

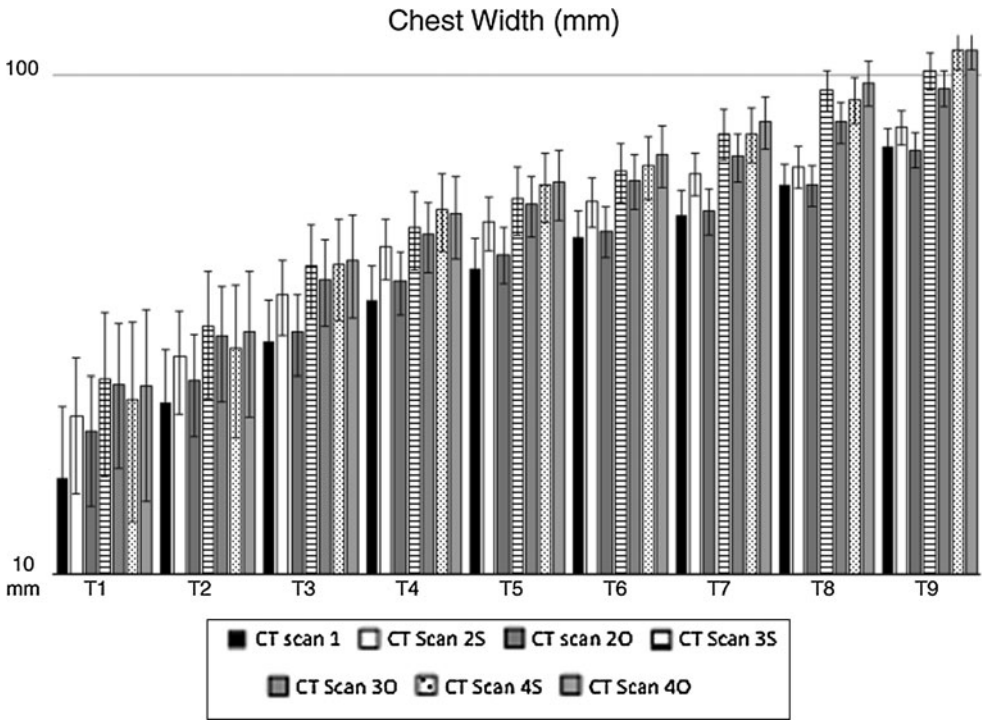

Fig. 6 Chest width (CW) changes from T1 to T9 in operated (O) and sham-operated (S) rabbits during the experiment. Mean values are expressed in millimeters (mm). *Error bars* identifies standard error. *CT Scan 1* CW before surgery (*black column*). Operated rabbits (O): *CT Scan 2O* CW 2 months after surgery, *CT Scan 3O* CW 6 months after surgery, *CT Scan 4O* CW 12 months after surgery. Sham-operated rabbits (S): *CT Scan 2S* CW 2 months after surgery, *CT Scan 3S* CW 6 months after surgery, *CT Scan 4S* CW 12 months after surgery

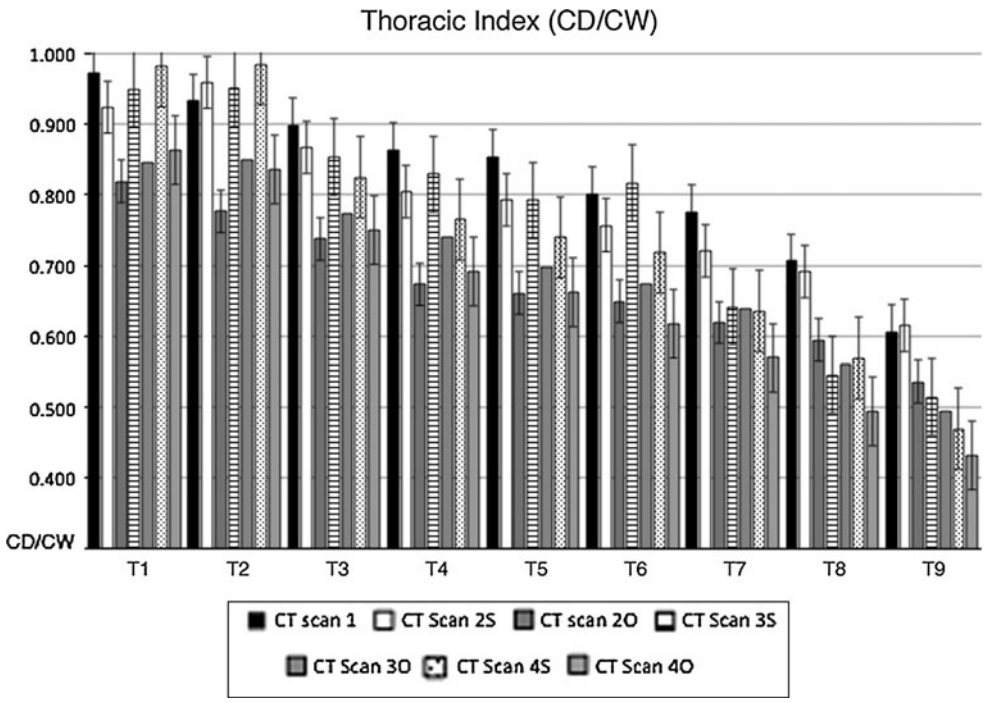

Fig. 7 Thoracic index (ThI) changes from T1 to T9 in operated (O) and sham-operated (S) rabbits during the experiment. *Error bars* identifies standard error. *CT Scan 1* (*CT1*) ThI before surgery (*black column*). Operated rabbits (O): *CT Scan 2O* ThI 2 months after surgery; *CT Scan 3O* ThI 6 months after surgery, *CT Scan 4O* ThI 12 months after surgery. Sham-operated rabbits (S): *CT Scan 2S* ThI 2 months after surgery, *CT Scan 3S* ThI 6 months after surgery, *CT Scan 4S* ThI 12 months after surgery.ThI was lower in operated compared to sham-operated rabbits, although not significantly different

%FS and EF ($p < 0.05$). Echocardiographic data were all within normal limits [35, 36].

Heart and lung measurements

Mean heart weight was 10 ± 1.6 g (range 7.2–11.5) in operated and 10.5 ± 1.4 g (range 8.6–12.1) in sham-operated animals; mean heart volume was 9.3 ± 1.8 mL (range 6.4–11.9) in operated and 10 ± 2.5 mL (range 6.7–13.4) in sham-operated animals. Mean weight of lungs was 18.6 ± 2.9 g (range 14.3–22.6) in operated and 17.5 ± 2.7 g (range 14.8–22) in sham-operated animals; mean lung volume was 21.1 ± 4.7 mL (range 16–29.5) in operated and 19.2 ± 3.1 mL (range 15.7–23.5) in sham-operated animals.

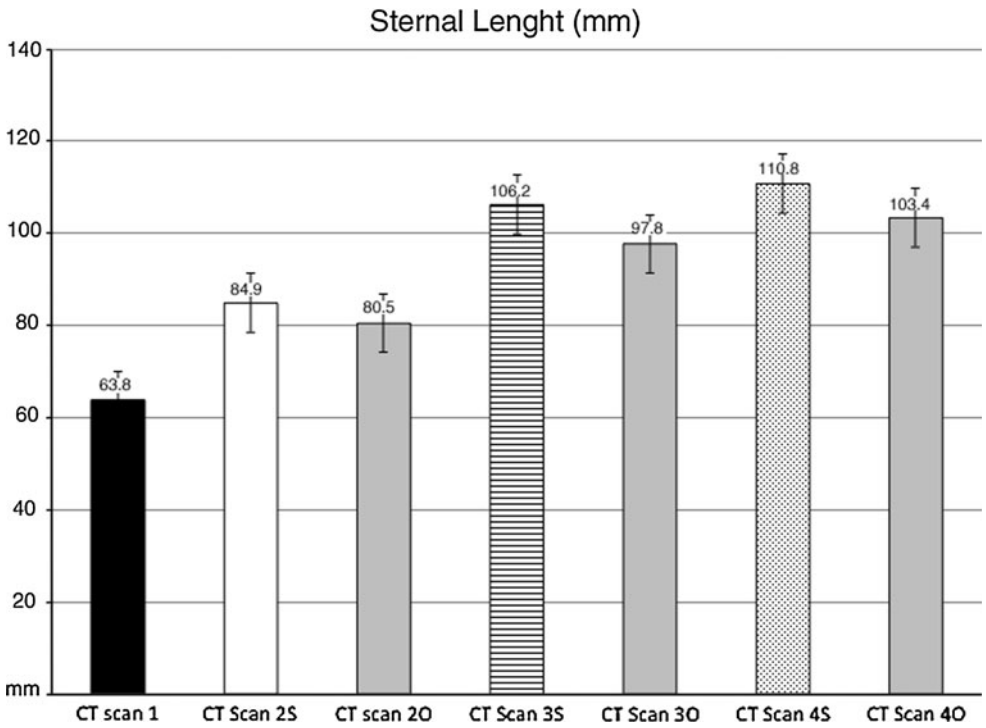

Fig. 8 Sternal length (StL) changes in operated and sham-operated rabbits during the experiment. Mean values are expressed in millimeters (mm). *Error bars* identifies standard error. *CT Scan 1* StL before surgery (*black column*). Operated rabbits (O): *CT Scan 2O* StL 2 months after surgery, *CT Scan 3O* StL 6 months after surgery, *CT Scan 4O* StL 12 months after surgery. Sham-operated rabbits (S): *CT Scan 2S* StL 2 months after surgery, *CT Scan 3S* StL 6 months after surgery, *CT Scan 4S* StL 12 months after surgery. *Table* and *graph* demonstrate that StL is reduced in operated rabbits. ThI was also lower in operated compared to sham-operated rabbits, although not significantly different. At completion of skeletal maturity, StL was reduced in operated compared to sham-operated rabbits ($p < 0.05$)

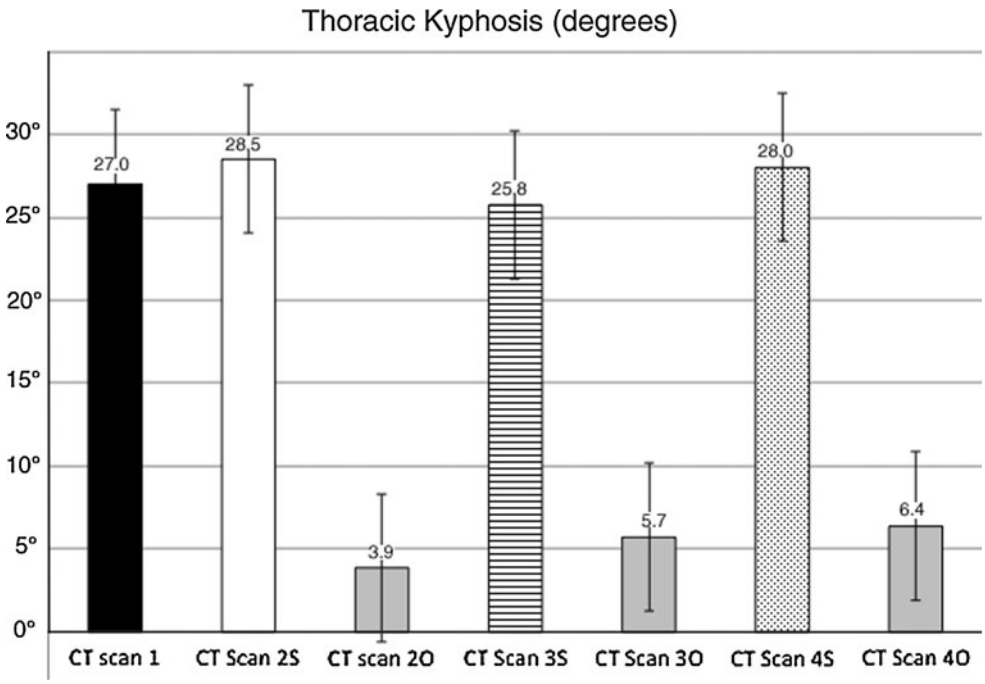

Fig. 9 Thoracic kyphosis (ThK) changes in operated and sham-operated rabbits during the experiment. Mean values are expressed in degrees (°). *Error bars* identifies standard error. *CT Scan 1* ThK before surgery (*black column*). Operated rabbits (O): *CT Scan 2O* ThK 2 months after surgery, *CT Scan 3O* ThK 6 months after surgery, *CT Scan 4O* ThK 12 months after surgery. Sham-operated rabbits (S): *CT Scan 2S* ThK 2 months after surgery, *CT Scan 3S* ThK 6 months after surgery, *CT Scan 4S* ThK 12 months after surgery. *Table* and *graph* demonstrate ThK is reduced in operated rabbits. At completion of skeletal maturity, ThK was reduced in operated compared to sham-operated rabbits ($p < 0.05$)

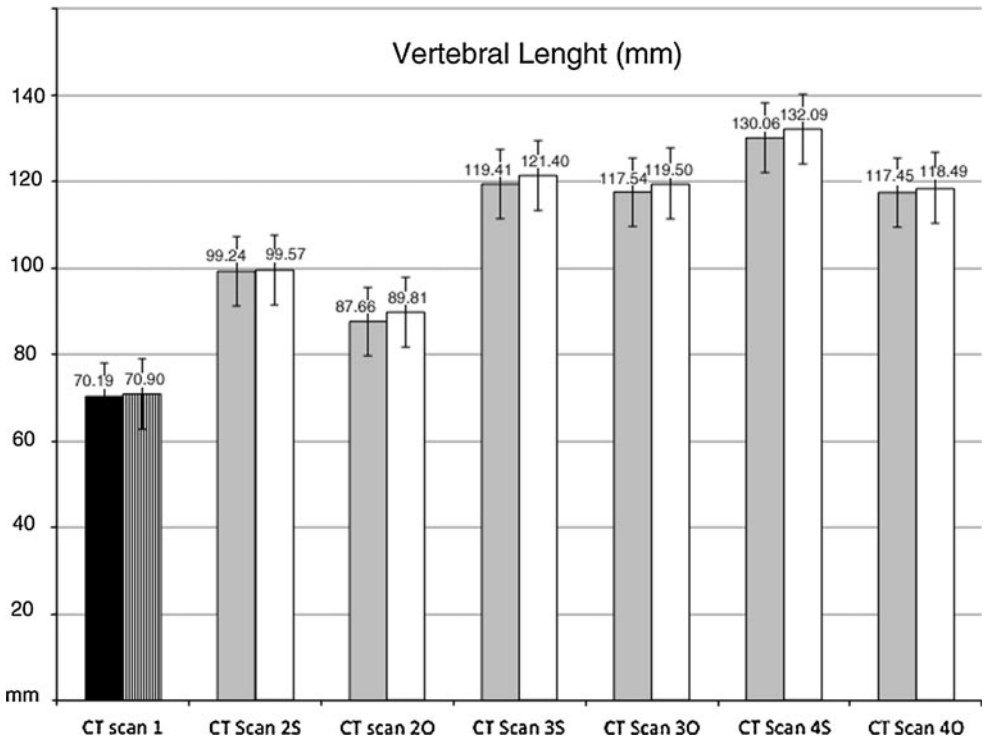

Fig. 10 Dorsal length (DL^{tot}) and ventral length (VL^{tot}) changes in operated and sham-operated rabbits during the experiment. DL^{tot} is represented by the *white column*; VL^{tot} is represented by the *grey column*. Mean values are expressed in millimeters (mm). *Error bars* identifies standard error. *CT Scan 1* DL^{tot} and VL^{tot} before surgery. Operated rabbits (O): *CT Scan 2O* DL^{tot} and VL^{tot} 2 months after surgery, *CT Scan 3O* DL^{tot} and VL^{tot} 6 months after surgery, *CT Scan 4O* DL^{tot} and VL^{tot} 12 months after surgery. Sham-operated rabbits (S): *CT Scan 2S* DL^{tot} and VL^{tot} 2 months after surgery, *CT Scan 3S* DL^{tot} and VL^{tot} 6 months after surgery, *CT Scan 4S* DL^{tot} and VL^{tot} 12 months after surgery. DL^{tot} and VL^{tot} are reduced in operated rabbits. DL^{tot}: *black columns*; VL^{tot}: *white columns*. At completion of skeletal maturity, DL^{tot} and VL^{tot} were reduced in operated compared to sham-operated rabbits ($p < 0.05$)

Table 2 Mean values ± SD of partial pressure of carbon dioxide ($PaCO_2$) in mmHg, partial pressure of oxygen (PaO_2) in mmHg, total carbon dioxide tension (TCO_2) in mEq/L, bicarbonates (HCO_3^-) in mmol/L, an oxygen saturation (sO_2) as a percentage (%) and pH

Parameter	Operated (mean ± SD)	Sham-operated (mean ± SD)	*p* value
$PaCO_2$ (mmHg)	29.2 ± 2.6	29.2 ± 1.7	0.1
PaO_2 (mmHg)	90 ± 18.2	98.3 ± 24.5	0.21
TCO_2 (mEq/L)	22.78 ± 4.18	21.33 ± 2.34	0.1
HCO_3^- (mmol/L)	21.8 ± 4.02	20.53 ± 2.36	0.11
sO_2 (%)	96.89 ± 2.37	97.83 ± 1.17	0.24
pH	7.46 ± 0.06	7.45 ± 0.06	0.18

Discussion

In this study, our experimental model aimed to evaluate the changes induced by thoracic spine arthrodesis on the thoracic cage shape and function of rabbits with non-deformed spine. Rabbits are sufficiently large, tolerate well GA and can be subjected to echocardiographic assessment [30–34] in the conscious state and allow easy blood withdrawals from artery and veins of the ears [13, 14, 23, 37–41]. Rabbits were prepubertal at the time of surgery and were followed for 1 year. Final measurments were performed 5 months after completion of skeletal growth. Thoracic cage shape was assessed on CT scan images. CT scans provide adequate images to allow the measurement of multiple thoracic cage parameters in arthrodesed rabbits [13, 14].

The thoracic cage can be defined as the space between the thoracic spine dorsally, the sternum ventrally and the ribs on both sides. Arthrodesis of the whole thoracic spine led to reduced CD, DL^{tot}, VL^{tot}, ThK and StL. Overall, the thoracic cage of operated rabbits grew less than that of sham-operated animals. In particular, CD decreased from 44.49 to 40.14 mm, DL^{tot} from 130.18 to 117.45 mm, VL^{tot} from 132.09 to 116.07 mm, ThK from 28° to 6.7°,

Table 3 Mean values ± SD for 2-dimensional and M-mode echocardiographic variables in 16 female NZW rabbits in the conscious state

Parameter	Operated (mean ± SD)	Sham-operated (mean ± SD)	*p* value
IVSd (mm)	3.06 ± 0.47	3.39 ± 0.33	0.11
IVSs (mm)	3.9 ± 0.33	4.29 ± 0.32	0.05
DVSd (mm)	16.68 ± 1.22	15.74 ± 1.55	0.47
DVSs (mm)	11.49 ± 2.15	11.44 ± 1.13	0.48
PPVSd (mm)	3.49 ± 0.41	3.53 ± 0.28	0.43
PPVSs (mm)	4.02 ± 0.65	4.23 ± 0.39	0.28
%FS	36 ± 4.67	29.71 ± 3.17	0.01
LA (mm)	10.82 ± 0.66	10.66 ± 0.95	0.39
EF (%)	68.78 ± 6.2	60.71 ± 6.33	0.04
Ao (mm)	8.16 ± 0.8	7.63 ± 0.43	0.12
LA/Ao	1.29 ± 0.11	1.31 ± 0.13	0.4
Ao Vel_{max} (m/s)	0.72 ± 0.14	0.79 ± 0.12	0.21
GP Ao_{max} (m/s)	2.22 ± 0.76	2.73 ± 0.85	0.17
Po Vel_{max} (m/s)	0.66 ± 0.11	0.68 ± 0.1	0.41
GP Po_{max} (m/s)	1.84 ± 0.58	1.93 ± 0.62	0.41

Thickness of the interventricular septum in diastole (IVSd) and systole (IVSs) in mm; left ventricular internal diameter in diastole (DVSd) and systole (DVSs) in mm; left ventricular free wall in diastole (PPVSd) and systole (PPVSs) in mm; contractile capacity of the left ventricle in mm (%FS); thickness of the left atrium in mm (LA); ejection fraction as a percentage (EF); thickness of the aortic wall (Ao) in mm; and LA/Ao ratio; maximal aortic outflow velocity (Ao Vel_{Max}) in m/s; maximal aortic outflow pressure gradient (GP Ao_{Max}) in mm of mercury (mmHg); maximal pulmonary outflow velocity in m/s (Po Vel_{Max}); maximal aortic outflow pressure gradient in mmHg (GP Po_{Max})

and StL from 110.83 to 103.05 mm, in sham-operated and operated rabbits, respectively (Figs. 5, 6, 7, 8, 9, 10). Thoracic cage growth irregularities secondary to thoracic spine arthrodesis did not alter all blood and echocardiographic parameters. However, operated rabbits showed a tendency to have greater PaO_2 reduction and $PaCO_2$ increase compared to sham-operated rabbits, thus highlighting a possible modification of gas exchanges. Furthermore, %FS and EF were significantly higher in operated rabbits, but remained within the normal range [36, 37]. Rabbits were housed in stainless steel cages, in compliance with national and international animal care regulations. However, the size of the cages and the subsequent relative inactivity of the animals may have impacted the clinical picture by limiting the effects of surgery in operated rabbits and by negatively influencing physiological results in sham-operated animals. Life expetancy of rabbits is about 4–5 years [42, 43]. In this experiment, animals were housed for 12 months and were euthanased at age 13 months.

In humans, untreated progressive early onset spinal deformities have been associated with short stature, short trunk and a deformed spinal column. The inability of the thorax to ensure normal breathing and the accompanying serious respiratory insufficiency is characterized by the TIS. This clinical picture can be linked to costo-vertebral malformations (e.g. fused ribs, hemivertebrae, congenital bars), neuromuscular disease (e.g. expiratory congenital hypotonia), syndromes such as Jeune and Jarcho-Levin, or to 50–5 % fusion of the thoracic spine before the age of 7 [1, 4–8, 44]. Thoracic cage size modification following spinal arthrodesis appears to be a progressive process involving multiple skeletal parameters simultaneously. In young children with progressive deformity, there is a decrease of longitudinal growth and a loss of the normal proportionality of trunk growth [5, 6, 10, 12]. As the spinal deformity progresses by a "domino effect", not only spinal growth is affected, but also the size and shape of the thoracic cage are modified. This distortion of the thorax will interfere with lung development. Over time, the scoliotic disorder changes in nature and from a mainly orthopaedic issue, it becomes a severe paediatric, systemic disorder with TIS, cor pulmonale, and reduced body mass index.

However, the clinical picture obtained with our experiment is not comparable to the one found in patients with severe and progressive spinal deformities. When TIS does occur in humans, loss of spinal height is extreme and secondary to spinal deformity. Karol et al. [5, 6] have shown also that a thoracic spine height of 18–22 cm or more is necessary to avoid severe respiratory insufficiency. Fusion is a cause of respiratory insufficiency and adds the loss of pulmonary function to the spinal deformity.

Moderate reduction of total spine length, reduction of ThK and absence of both scoliosis and crankshaft phenomenon characterized our experimental model. Current data corroborate data of works previously published [13, 16, 17, 19, 20]. It appears that moderate and progressive chest volume reduction should be differentiated from

severe and deregulated distortion and deformation of the trunk secondary to progressive spinal deformities. Scoliosis remains at the heart of severe chest deformities.

Our data support the idea that vertebral arthrodesis of a non-scoliotic spine induces mild to moderate chest deformities. The thoracic spine is the posterior pillar of the thoracic cage and, in humans, it measures about 12 cm at birth, 18 cm at 5 years of age and about 27 cm on average at skeletal maturity. In humans, thoracic cage shape varies with age. At birth, the difference between thoracic depth and width is minimal and thoracic depth/thoracic width ratio is very close to 1. Conversely, at skeletal maturity, the thoracic depth/thoracic width ratio is lower than 1 as width has grown more than depth. For this reason, the overall thoracic cage shape evolves from ovoid at birth to elliptical at skeletal maturity. At the end of growth, the thorax has an average thoracic depth of 21 cm in boys and 17.7 cm in girls with an average thoracic width of 28 and 24.7 cm, respectively [45–47].

In rabbits, on the other hand, the thoracic cage is fairly conical from birth to skeletal maturity. In operated rabbits, the thoracic cage changed its morphology following dorsal arthrodesis. The vertebral fusion involved all thoracic vertebrae and the effects on the growth of the thorax which, with a lower growth of chest depth (CD) and an increased chest width (CW), changed from a fairly circular shape to one that tends to be elliptical, were particularly evident. Moreover, at completion of skeletal maturity, rabbits having undergone a precocious spinal fusion showed a 10 % shorter T1–T12 segment compared to sham-operated subjects [45–48].

Our experimental model does not support the hypothesis that a precocious arthrodesis of a non-deformed spine could be source of cardiopulmonary complications [1, 3–5, 9, 10, 12] severe enough to reproduce a clinical picture comparable to TIS.

Thoracic cage growth irregularities secondary to thoracic spine arthrodesis did not alter all blood and echocardiographic parameters. Therefore, it is possible that to develop TIS or similar clinical pictures, a deformed spine and significantly reduced spinal height must be present simultaneously.

Our conclusion is that thoracic spine arthrodesis in prepubertal rabbits with non-deformed spine does not alter the plastic properties of the thorax. Thoracic cage modifications are expression of the maintained plasticity of the thorax even in presence of an arthrodesed spine. Loss of ThK and moderate reduction of thoracic spine length are compensated by an increased chest width.

To obtain more relevant information to TIS, this experimental study should be repeated after creating a scoliostic deformity or rib fusion in the immature rabbits. We consider adding the following, yet another speculation: it is theoretically possible that chronicity is another factor of some impact; in other words, we had allowed for more than 12 months to pass post-operatively the reported changes we have seen would have progressed even further, potentially enough to show statistical significance.

Conflict of interest None.

References

1. Swank SM, Winter RB, Moe JH (1982) Scoliosis and cor pulmonale. Spine 7:343–354
2. Winter RB, Lonstein JE (1999) Congenital scoliosis with posterior spinal arthrodesis T2–L3 at age 3 years with 41 years follow-up. Spine 24:194–197
3. Campbell RM, Smith MD, Mayes TC et al (2003) The characteristics of thoracic insufficiency associated with fused ribs and congenital scoliosis. J Bone Joint Surg Am 85:409–420
4. Goldberg CJ, Gillic I, Connaughton O et al (2003) Respiratory function and cosmesis at maturity in infantile-onset scoliosis. Spine 28:2397–2406
5. Karol LA, Johston C, Mladenov K et al (2008) Pulmonary function following early thoracic fusion in non neuromuscular scoliosis. J Bone Joint Surg Am 90:1272–1281
6. Karol LA (2011) Early definitive spinal fusion in young children: what we have learned. Clin Orthop Relat Res 469(5):1323–1329
7. Dubousset J, Wicart P, Pomero V et al (2003) Spinal penetration index: new three-dimensional quantified reference for lordoscoliosis and other spinal deformities. J Orthop Sci 8(1):41–49
8. Dubousset J (1973) Recidive d'une scoliose lombaire et d'un basin oblique après fusion précoce: le phénomène du Villebrequin. Proceeding Group Etude de la Scoliose, Paris
9. Dubousset J, Herring JA, Shuffenbarger H (1989) The crankshaft phenomenon. J Pediatr Orthop 9:541
10. Campbell MR, Hell-Vocke AK (2003) Growth of the thoracic spine in the congenital scoliosis after expansion thoracoplasty. J Bone Joint Surg Am 85:409–420
11. Lee CS, Nachemson AL (1997) The crankshaft phenomenon after posterior Harrington fusion in skeletally immature patients with thoracic or thoracolumbar idiopathic scoliosis followed to maturity. Spine 22(1):2558–2567
12. Hefti FL, McMaster MJ (1983) The effect of the adolescent growth spurt on early posterior spinal fusion in infantile and juvenile idiopathic scoliosis. J Bone Joint Surg Br 65:247–254
13. Canavese F, Dimeglio A, Volpatti D et al (2007) Dorsal arthrodesis of thoracic spine and effects on thorax growth in prepubertal New Zealand white rabbits. Spine 32:E443–E450
14. Canavese F, Dimeglio A, Granier M et al (2008) Influence de l'arthrodèse vertébrale sélective T1–T6 sur la croissance thoracique: étude expérimentale chez des lapins New Zealand white prépubertaires. Rev Chir Orthop App Locom 94:490–497
15. Coleman SS (1960) The effect of posterior spinal fusion on vertebral growth in dogs. J Bone Joint Surg Am 50:879–896
16. Ottander HG (1963) Experimental progressive scoliosis in a pig. Acta Orthop Scand 33:91–97
17. Veliskakis K, Levine DB (1966) Effect of posterior spine fusion on vertebral growth in dogs. J Bone Joint Surg Am 48:1367–1376
18. Ponseti IV, Friedman B (1950) Changes in the scoliotic spine after fusion. J Bone Joint Surg Am 32:751–766
19. Canavese F, Dimeglio A, Granier M et al (2007) Arthrodesis of the first six dorsal vertebrae in prepubertal New Zealand white rabbits and thoracic growth to skeletal maturity: the role of the

"Rib-Vertebral-Sternal complex". Minerva Ortop Traumatol 58:369–378
20. Canavese F, Dimeglio A, D'Amato C et al (2010) Dorsal arthrodesis in prepubertal New Zealand white rabbits followed to skeletal maturity: effect on thoracic dimensions, spine growth and neural elements. Indian J Orthop 44:14–22
21. Lowe TG, Wilson L, Chien JT et al (2005) A posterior tether for fusionless modulation of sagittal plane growth in a sheep model. Spine 30:S69–S74
22. Mehta HP, Snyder BD, Baldassarri SR et al (2011) Expansion thoracoplasty improves respiratory function in a rabbit model of postnatal pulmonary hypoplasia: a pilot study. Spine 35:153–161
23. Mehta HP, Snyder BD, Callender NN et al (2006) The reciprocal relationship between thoracic and spinal deformity and its effect on pulmonary function in a rabbit model: a pilot study. Spine 31:2654–2664
24. Moon MS, Ok IY (1980) The effect of posterior spinal fixation with bone cement upon vertebral growth in dogs. Int Orthop 4:13–18
25. Kilkenny C, Browne WJ, Curthill IC et al (2010) Improving bioscience research reporting: the ARRIVE guidelines for reporting animal research. PLoS Biol 8(6):e1000412. doi: 10.137/journal.pbio.1000412
26. Resina J, Ferriera-Alves A (1977) A technique of correction and internal fixation for scoliosis. J Bone Joint Surg Br 59:159–164
27. Drummond DS (1998) Harrington instrumentation with spinous process wiring for idiopathic scoliosis. Orthop Clin North Am 19(2):281–289
28. Barone R (1980) Anatomia comparata dei Mammiferi domestici [Italian edition by Bortolami R]. Edagricole, Bologna
29. Cobb JR (1948) Outline for the study of scoliosis. Instrictinal Course Lectures 5:261–275
30. Szabuniewicz M, Hightower D, Kyraz JR (1971) The electrocardiogram, vectocardiogram and spatiocardiogram in the rabbit. Can J Comp Med 35:107–114
31. Cheitlin M, Alpert J, Amstrong W (1997) ACC/AHA guidelines for the clinical application of echocardiography. Circulation 95:1686–1774
32. Fontes-Sousa AP, Bras-Silva C, Moura C et al (2006) M-mode and Doppler echocardiographic reference values for male New Zealand white rabbits. Am J Vet Res 67:1725–1729
33. Stypmann J, Engelen MA, Breithardt AK et al (2007) Doppler echocardiography and tissue Doppler imaging in the healthy rabbit: differences of cardiac function during awake and anaesthetised examination. Int J Cardiol 115:164–170
34. Thomas WP, Gaber CE, Jacobs GJ et al (1993) Recommendations for standards in transthoracic two-dimensional echocardiography in the dog and cat. Echocardiography Committee of the Specialty of Cardiology, American College of Veterinary Internal Medicine. J Vet Intern Med 7:247–252
35. Fontes-Sousa AP, Moura C, Santos Carneiro C et al (2009) Echocardiographic evaluation including tissue Doppler imaging in New Zealand white rabbits sedated with ketamine and midazolam. Vet J 181:326–331
36. Noszczyk-Nowak A, Nicpon J et al (2009) Preliminary reference values for electrocardiography, echocardiography and myocardial morphometry in the European brown hare (*Lepus europaeus*). Acta Vet Scand 51:6
37. Bras-Silva C, Fontes-Sousa AP, Moura C et al (2006) Impaired response to ET(B) receptor stimulation in heart failure: functional evidence of endocardial endothelial dysfunction? Exp Biol Med 231:893–898
38. Martin MW, Darke PG, Else RW (1987) Congestive heart failure with atrial fibrillation in a rabbit. Vet Rec 121:570–571
39. Marco I, Cuenca R, Pastor J et al (2003) Hematology and serum chemistry values in the European brown hare. Vet Clin Pathol 32:185–198
40. Noszczyk-Nowak A, Paslawske U, Zysko D et al (2007) Cardiac hypertrophy induced by administration of oral L-thyroxine in growing pigs. Medycyna Weterynarya 63:113–117
41. Pikula J, Adam V, Bandouchova H et al (2007) Blood coagulation times in the European brown hare (*Lepus europaeus*). Vet Clin Pathol 36:361–363
42. Janssen M, de Wilde RF, Kouwenhoven JWM et al (2011) Experimental animal models in scoliosis research: a review of the literature. Spine J 11(4):347–358
43. Kawakami N, Deguchi M, Kanemura T (1999) Animal models in scoliosis. In: An YH, Friedman RJ (eds) CRC Press. FL, Boca Raton, pp 549–564
44. Rizzi PE, Winter RB, Lonstein JE et al (1997) Adult spinal deformity and respiratory failure. Surgical results in 35 patients. Spine 22:2517–2530
45. Dimeglio A (2005) Growth in pediatric orthopaedics. In: Morrissy T, Weinstein SL (eds) Lovell & Winter's pediatric orthopaedics, 6th edn. Lippincott William & Wilkins, Philadelphia, pp 35–65
46. Dimeglio A (1993) Growth of the spine before age 5 years. J Pediatr Orthop B 1:102–107
47. Dimeglio A, Bonnel F (1990) Le rachis en croissance. Springer, Paris
48. Moon MS, Ok IY, Ha KY (1986) The effect of posterior spinal fixation with acrylic cement on the vertebral growth plate and intervertebral disc in dogs. Int Orthop 10:69–73